Chemistry and Physics of Lipids 212 (2018) 80–87

Contents lists available at ScienceDirect

Chemistry and Physics of Lipids

journal homepage: www.elsevier.com/locate/chemphyslip

Perdeuteration of cholesterol for neutron scattering applications using recombinant *Pichia pastoris*

Martine Moulin[a,b,1], Gernot A. Strohmeier[c,d,1], Melanie Hirz[e,1], Katherine C. Thompson[f], Adrian R. Rennie[g], Richard A. Campbell[a], Harald Pichler[c,e], Selma Maric[h], V. Trevor Forsyth[a,b], Michael Haertlein[a,*]

[a] Institut Laue-Langevin, 71, Avenue des Martyrs, Grenoble 38042, France
[b] Faculty of Natural Sciences, Keele University, Keele, Staffordshire ST5 5BG, United Kingdom
[c] acib, Austrian Centre of Industrial Biotechnology GmbH, 8010 Graz, Austria
[d] Institute of Organic Chemistry, NAWI Graz, Graz University of Technology, 8010 Graz, Austria
[e] Institute of Molecular Biotechnology, NAWI Graz, BioTechMed Graz, Graz University of Technology, 8010 Graz, Austria
[f] Department of Biological Sciences and Institute of Structural and Molecular Biology, Birkbeck College, University of London, Malet Street, London WC1E 7HX, United Kingdom
[g] Centre for Neutron Scattering, Uppsala University, 751 20 Uppsala, Sweden
[h] Biofilms – Research Centre for Biointerfaces and Biomedical Science Department, Faculty of Health and Society, Malmö University, Malmö 20506, Sweden

ARTICLE INFO

Keywords:
Perdeuteration
Cholesterol
Pichia pastoris
Neutron scattering
Lipid engineering

ABSTRACT

Deuteration of biomolecules has a major impact on both quality and scope of neutron scattering experiments. Cholesterol is a major component of mammalian cells, where it plays a critical role in membrane permeability, rigidity and dynamics, and contributes to specific membrane structures such as lipid rafts. Cholesterol is the main cargo in low and high-density lipoprotein complexes (i.e. LDL, HDL) and is directly implicated in several pathogenic conditions such as coronary artery disease which leads to 17 million deaths annually. Neutron scattering studies on membranes or lipid-protein complexes exploiting contrast variation have been limited by the lack of availability of fully deuterated biomolecules and especially perdeuterated cholesterol. The availability of perdeuterated cholesterol provides a unique way of probing the structural and dynamical properties of the lipoprotein complexes that underly many of these disease conditions. Here we describe a procedure for *in vivo* production of perdeuterated recombinant cholesterol in lipid-engineered *Pichia pastoris* using flask and fed-batch fermenter cultures in deuterated minimal medium. Perdeuteration of the purified cholesterol was verified by mass spectrometry and its use in a neutron scattering study was demonstrated by neutron reflectometry measurements using the FIGARO instrument at the ILL.

1. Introduction

Neutron scattering studies offer unique insights to structural biology, especially when used in conjunction with selective and non-selective deuteration approaches (Haertlein et al., 2016). In neutron crystallography, hydrogen atoms are readily visible, yielding crucial information on protonation states of active site residues, charge transfer processes, and hydration (Howard et al., 2011; Cuypers et al., 2013a,b; Casadei et al., 2014; Haupt et al., 2014; Blakeley et al., 2015; Cuypers et al., 2016; Kwon et al., 2016). Small-angle neutron scattering (SANS) studies have the significant advantage that contrast variation methods can be used to distinguish and model different components of a macromolecular complex (Vijayakrishnan et al., 2010; Cuypers et al., 2013a,b; Ibrahim et al., 2017, Appolaire et al., 2014, Edlich-Muth et al., 2015), and in a comparable way, neutron reflection studies allow strongly complementary information to be provided in the analysis of membranous interfaces (Grage et al., 2011; Fragneto, 2012). Furthermore, important aspects of macromolecular dynamics and its coupling to hydration water dynamics are provided by neutron incoherent scattering studies (Schirò et al., 2015). These insights result mainly from the fact that the scattering powers for neutrons of both hydrogen and deuterium are of comparable magnitude (although, crucially, their scattering lengths differ in sign) with those of the other atoms typically found in biological macromolecules - in strong contrast to the situation

* Corresponding author.
E-mail address: haertlein@ill.fr (M. Haertlein).
[1] These authors contributed equally to this work.

https://doi.org/10.1016/j.chemphyslip.2018.01.006
Received 16 October 2017; Received in revised form 20 December 2017; Accepted 15 January 2018
Available online 31 January 2018

for X-rays where hydrogen/deuterium atoms scatter very weakly. This is of crucial importance given that about half of the atoms in biological molecules are hydrogen and that they are often highly significant to biological structure, dynamics, and function. Deuteration, the replacement of hydrogen atoms by the stable isotope deuterium, is a powerful method for the investigation of the structure and dynamics of biomolecules by means of NMR, Raman/infrared spectroscopy and neutron scattering. In the case of neutron analyses, the pronounced differences between the scattering lengths of hydrogen- and deuterium-containing molecules enable parts of molecular complexes to be highlighted by neutron scattering methods such as small-angle neutron scattering (SANS), neutron reflectometry (NR), or neutron crystallography (NMX).

In the case of structural work on lipid systems by SANS and NR as well as NMR (Stockton et al. (1977); Hagn et al. (2013), the deuteration of phospholipids and other membrane components can be heavily exploited (Maric et al., 2014; de Ghellinck et al., 2014; Gerelli et al., 2014; Foglia et al., 2011). However, chemical synthesis of unsaturated perdeuterated lipids and sterols still remains challenging. de Ghellinck et al. (2014) have demonstrated that perdeuterated phospholipids and sterols can be extracted from *P. pastoris* cells grown in deuterated minimal medium. These authors have also shown that while the phospholipid and ergosterol homeostasis is maintained in deuterated cultures, the fatty acid unsaturation level is modified; the production of perdeuterated unsaturated lipids is significantly enhanced when *P. pastoris* is grown at lower temperatures.

The multi-lamellar organization of fully deuterated lipid extracts of *P. pastoris* membranes has been shown using neutron diffraction (Gerelli et al., 2014). This study showed that at high relative humidity, non-deuterated and deuterated lipids are similar in their multi-lamellar organization. However, at low relative humidity, non-deuterated lipids are characterized by a larger single lamellar structure than observed for the deuterated samples. Furthermore, perdeuterated lipids have been used to characterize structural changes in the membrane of *P. pastoris* induced by the antifungal Amphotericin B (de Ghellinck et al., 2015).

In addition to the extraction of lipids from non-recombinant *P. pastoris* cultures, perdeuterated lipids have also been isolated from non-recombinant *E. coli* (Lind et al., 2015) and a recombinant *E. coli* expression system was successfully used for the biosynthesis of selectively deuterated phosphatidylcholine (PC) (Maric et al., 2014, Maric et al., 2015).

Chemically synthesised cholesterol molecules that are partially deuterated − such as cholesterol-D_6 (deuteration in ring) and cholesterol-D_7 (deuteration in tail) are commercially available (Kessner et al., 2008). However, fully deuterated cholesterol (cholesterol-D_{46}) is difficult to synthesize chemically. Since high concentrations of deuterium are toxic for mammals and mammalian cell lines, perdeuteration of cholesterol cannot be achieved in native organisms. A biosynthetic route for this therefore depends on the use of a deuterium-resistant recombinant organism that can be adapted to growth in a fully deuterated medium. *P. pastoris,* a methylotrophic yeast, has been shown to grow in fully deuterated minimal medium with d_8-glycerol as carbon source and to produce perdeuterated lipids including ergosterol, a molecule related to cholesterol (Haertlein et al., 2016; de Ghellinck et al., 2014; Hirz et al., 2013) have succeeded in lipo-engineering *P. pastoris* by several gene insertions and knock-out mutations to produce cholesterol instead of its native ergosterol. Here, we report a robust protocol for recombinant perdeuteration of cholesterol in a lipo-engineered *P. pastoris* strain in flask and in high cell-density cultures. The biosynthetically labelled cholesterol has been produced and purified in large quantities (tens of mg). The production, HPLC purification, and characterisation by gas chromatography and mass spectrometry are described. An example illustrating the feasibility of exploiting the perdeuterated d-cholesterol in neutron scattering studies is demonstrated by NR measurements from perdeuterated and unlabelled cholesterol in a synthetic lipid monolayer.

2. Materials and methods

2.1. Growth of recombinant P. pastoris in perdeuterated flask cultures

The cholesterol producing strain CBS7435 *Δhis4 Δku70 Δerg5*:pPpGAP-Zeocin™-[DHCR7] *Δerg6*:pGAP-G418[DHCR24] (Hirz et al., 2013) was first grown in YPD medium (1% yeast extract, 2% peptone, 2% glucose, 300 mg/l geneticin sulfate and 100 mg/l Zeocin™). This pre-culture was used to inoculate a culture in basal salts medium (BSM): 38.1 g/l H_3PO_4, 0.93 g/l $MgSO_4$, 4.13 g/l KOH, 40 g/l glycerol, 4×10^{-5}% biotin, 2×10^{-3}% histidine, 300 mg/l geneticin sulfate, 100 mg/l Zeocin™ and 4.35 ml/l PTM1 trace salts. The composition of PTM1 trace salts was the following: cupric sulphate pentahydrate 6 g/l, sodium iodide 0.08 g/l, manganese sulphate monohydrate 3.0 g/l, sodium molybdate dihydrate 0.2 g/l, boric acid 0.02 g/l, cobalt chloride 0.5 g/l, zinc chloride 20.0 g/l, ferrous sulphate heptahydrate 65.0 g/l, biotin 0.2 g/l, sulphuric acid, 5 ml/l. The deuterated medium was prepared in the following way: 1 l of non-deuterated BSM without glycerol was flash evaporated, the powder was resuspended in 250 ml of 99.85% D_2O (Euriso-top) and flash evaporated again. This process was repeated twice to get rid of trace H_2O. Finally, the powder was resuspended in 1 l D_2O (purity > 99.9%,) containing 40 g d_8-glycerol (Euriso-top).

900 ml of deuterated BSM were inoculated with 100 ml of a starting culture (OD_{600} of about 20). The culture was incubated at 29 °C under shaking at 200 rpm and harvested after 10 days. A final OD_{600} of about 30 corresponding to 25 g of *Pichia* cellular wet weight was obtained.

2.2. Growth of recombinant P. pastoris in perdeuterated fed-batch cultures

900 ml of deuterated BSM containing 10 g of d_8-glycerol was inoculated with 100 ml of preculture in a 3 l fermenter (Labfors, Infors). During the batch and fed-batch phases the pD was adjusted to 6.0 by the addition of NaOD and the temperature was adjusted to 28 °C. The gas-flow rate of sterile filtered air was 2.0 l/min. Stirring was adjusted to ensure a dissolved oxygen tension (DOT) of 30%. The initial OD_{600} was 0.9. After 7 days the glycerol from the batch phase was consumed and the fed-batch phase was initiated by constant feeding of 30 g of d_8-glycerol over 12 days. The final OD_{600} was 40 and 32 g of *Pichia* cellular wet weight was obtained.

2.3. Determination of sterol production

15 mg of deuterated or non-deuterated *Pichia* cell paste was transferred to Pyrex tubes and resuspended in 1 ml of 0.2% pyrogallol in MeOH and 400 µl of 60% KOH. Five µl of ergosterol (2 mg/ml) were added as internal standard (IS) and samples were saponified at 90 °C for 2 h. Sterols were extracted three times with *n*-heptane and dried under a stream of nitrogen. Dried extracts were dissolved in 10 µl of pyridine and derivatized with 10 µl of *N'O'*-bis(trismethylsilyl)-trifluoracetamide. Samples were diluted with 50 µl of ethyl acetate and analyzed by gas chromatography–mass spectrometry (GC–MS) (Hirz et al., 2013).

2.4. Isolation and purification of perdeuterated cholesterol

Cholesterol was extracted from *P. pastoris* cell paste using an organic solvent extraction procedure. The cell paste was transferred into a 500 ml round-bottomed flask to which was added 65 g potassium hydroxide, 43 ml water, 200 ml methanol and 350 mg pyrogallol. This mixture was heated for 3 h under gentle reflux while keeping the stirring at a minimum to avoid foaming. After cooling to room temperature, insoluble materials were filtered off and the methanolic solution was extracted three times - each with 100 ml cyclohexane. The combined extracts were washed with 100 ml water, dried over sodium sulphate and concentrated under reduced pressure. The crude material

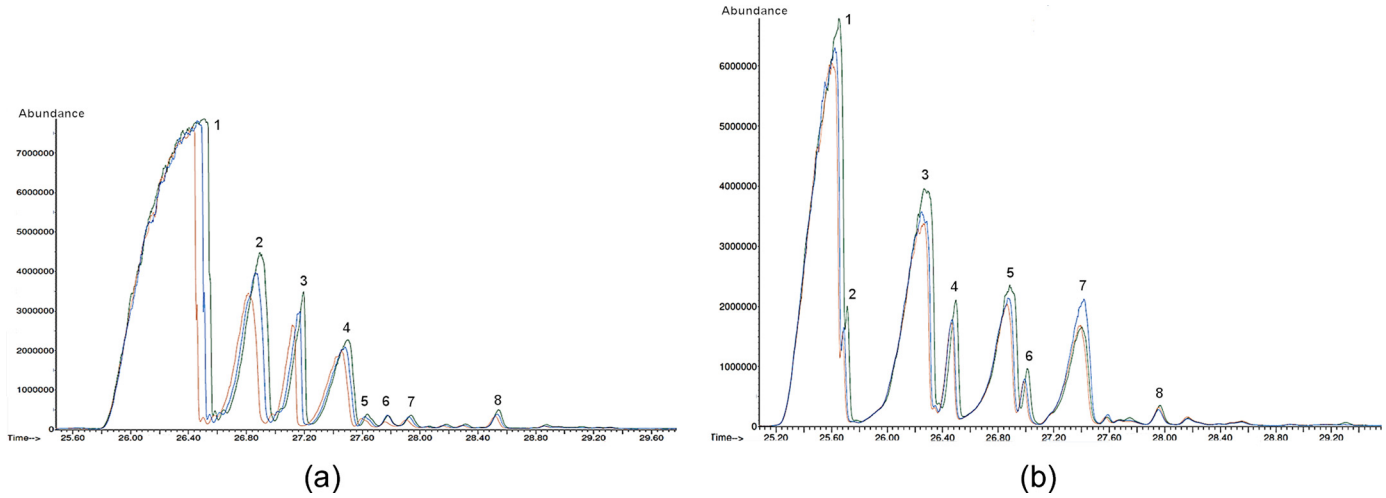

Fig. 1. Gas chromatography-mass spectrometry (GC–MS) analysis showing sterol components in (a) unlabelled and (b) perdeuterated flask cultures. Each measurement was repeated 3 times (green, red and blue curves). The various peaks indicated are identified in Table 1. The main component is clearly cholesterol, but other sterols are identified such as 7-DHC and zymosterol. (For interpretation of the references to colour in this figure legend, the reader is referred to the web version of this article.)

was treated with 10 ml ethyl acetate and passed through a short plug of silica gel to remove polar impurities and insoluble materials. The perdeuterated cholesterol was isolated in pure form using a ThermoFisher UltiMate 3000 binary semipreparative HPLC system equipped with a NUCLEODUR® 100-10 C18ec column (125 mm × 21 mm, 5 µm, Macherey-Nagel, Düren, Germany) and a VP 20/16 NUCLEODUR® C18ec guard column. Using an isocratic mixture consisting of acetonitrile/methanol (9:1) at a flow rate of 20 ml/min at 30 °C using a detection wavelength of 210 nm, the desired product was collected baseline-separated between 18.7 and 25.0 min. After removing the solvent under reduced pressure, pure perdeuterated cholesterol was obtained. HPLC analysis was conducted on an Agilent 1100, equipped with a DAD detector and a NUCLEODUR® C18 Gravity column (150 mm × 3 mm, 3 µm, Macherey-Nagel, Düren, Germany) using an isocratic mixture of acetonitrile/methanol 1:1 at a flow rate of 0.70 ml/min at 30 °C.

2.5. Neutron reflectometry measurements

NR measurements were carried out using the FIGARO instrument at the Institut Laue-Langevin (ILL) (Campbell et al., 2011). Data were recorded using neutrons with wavelengths of 2–30 Å at incident angles of 0.62° and 3.8°. Data from three samples were recorded to illustrate the effect of replacing the h-cholesterol by d-cholesterol. A mixture of 1:4 cholesterol to dipalmitoylphosphatidylcholine (DPPC) by mole was prepared in each case as a chloroform solution. After spreading and compression to a surface pressure of 25 mN m^{-1}, the reflectivity was measured, which was normalized with respect to a measurement of pure D_2O. Three neutron contrasts were studied (i) h-cholesterol with d_{62}-DPPC on null reflecting water (NRW), (ii) h-cholesterol with d_{62}-DPPC on D_2O and (iii) d-cholesterol with h-DPPC on NRW, where NRW is a mixture of 8.1% v/v D_2O in H_2O that has zero scattering length density. Data fitting was carried out using a two layer model of tails and hydrated lipid head, with the cholesterol included in the tail layer. A two-layer model was applied where the one in contact with air comprised the acyl chains of the lipid together with cholesterol, and the one in contact with the water comprised solvated head groups. The number of chains was constrained to be equal to the number of head groups of the phospholipid in the layers and the surface excess of the lipid and of the cholesterol were constrained to be equal in the three measured contrasts. The scattering length density of the d-cholesterol was taken as 7.65×10^{-6} Å^{-2}, h-cholesterol as 0.21×10^{-6} Å^{-2}, the tails of d_{62}-DPPC to 8.15×10^{-6} Å^{-2}, the tails of h-DPPC to -0.43×10^{-6} Å^{-2} and the heads of DPPC to 1.85×10^{-6} Å^{-2}. Note that the value of 8.15×10^{-6} Å^{-2} was calculated for the lipid tails ($C_{30}D_{62}$) for the d_{62}-DPPC using a volume for the tails corresponding to the liquid condensed phase (752 Å^3, Small, 1984; Marsh, 2010). Recent papers have followed such an approach (Micciulla et al., 2018; Sheridan et al., 2017; Braun et al., 2017). The d_{62}-DPPC was obtained from Avanti Polar lipids.

3. Results

3.1. Cell growth

The cholesterol producing *P. pastoris* strain was grown in unlabelled as well as in deuterated basal salt medium with d_8-glycerol as carbon source. A similar approach has been used by de Ghellinck et al. (2014) to produce perdeuterated non-recombinant yeast lipids. The growth behaviour of both the yeast lipid producing and the lipo-engineered cholesterol producing deuterated *Pichia* cultures showed a longer lag-phase in D_2O containing medium by comparison with cultures grown in unlabelled media. This was even more pronounced for the cholesterol producing culture (4 vs. 2 days). The growth rate in the exponential phase was the same for the perdeuterated and the unlabelled cholesterol producing cultures and a final OD_{600} of about 30 was obtained after 10 days. The non-recombinant yeast lipid producing cultures reached higher OD_{600} values (about 80 vs. 30) with shorter doubling times – indicating the growth inhibiting effect of cholesterol production in *P. pastoris* grown in deuterated minimal media.

3.2. Sterol analysis – deuterated versus non-deuterated samples

Samples of the unlabelled (control) and perdeuterated cholesterol producing *P. pastoris* cell paste from flask cultures were analysed by gas chromatography-mass spectrometry (GC–MS) for their sterol composition as described above. Deuterated sterols show a shorter retention time (between 0.6 and 0.9 min) by comparison with their non-labelled analogues, in accordance with the published data on perdeuterated ergosterol produced in *P. pastoris*. Fig. 1 shows the gas chromatogram for the sterols produced by the strain (*i.e.* cholesterol, 7-dehydroxycholesterol (7-DHC) and zymosterol) under both non-deuterated (Fig. 1(a)), and deuterated (Fig. 1(b)) conditions. Tables 1a and 1b show the sterol compositions of both unlabelled and perdeuterated cholesterol-producing *P. pastoris* cell pastes. The largest observed mass was 503 Da as expected for trimethylsilylated perdeuterated cholesterol. In the deuterated samples, additional peaks occur, which relate to intermediates in the sterol biosynthetic pathway. These compounds may arise as a result of a lower activity of deuterated DHCR7 (7-dehydrocholesterol reductase), DHCR24 (24-dehydrocholesterol reductase) and *ERG24* (C-14 sterol reductase) enzymes. The results indicate that cholesterol

Table 1a
Sterol composition of unlabelled cholesterol-producing *P. pastoris* cell paste (mean values ± SD of triplicates are shown). Ergosterol was used as an internal standard (IS).

Peak	Compound	Retention time (RT) (min)	Rel. RT	Peak area	% of total sterols	µg
1	Cholesterol	26.464	1.000	2027067085	76.6 ± 0.4	100 ± 5
2	7-dehydrocholesterol (7-DHC)	26.858	1.015	400667110	15.1 ± 0.3	20 ± 2
3	Zymosterol	27.161	1.026	168125109	6.3 ± 0.1	8 ± 1
4	Ergosterol (IS)	27.480	1.038	202332149		10
5	Cholesta-7,24(25)-dienol	27.619	1.044	13599901	0.5 ± 0.0	1 ± 0
6–8	not identified			39377438	1.5 ± 0.1	2 ± 0
Total sterols		8.4 ± 0.4 mg/g CWW				

biosynthesis may not occur as efficiently in deuterated media as it does in unlabelled growth media; this is also reflected in the lower amounts of total sterols extracted from the deuterated cell paste (see Table 1b). The molecular structures of the main sterol species synthesized in *P. pastoris* under non-deuterated and deuterated conditions are shown in Fig. 2.

With a cholesterol content greater than 50% of total sterols and a total sterol production of about 6 mg per gram of *Pichia* wet weight (CWW), the sterol analysis clearly demonstrates the feasibility of producing significant amounts of perdeuterated cholesterol using recombinant *P. pastoris* (> 3 mg/g cellular wet weight).

3.3. The effect of flask/fermenter cultures on deuterated sterol production

Since deuterated media components such as D_2O and d_8-glycerol are costly, the possibility of using deuterated high-cell density cultures as a cost efficient alternative to flask cultures was investigated. A fed-batch culture was grown using deuterated minimal medium and a d_8-glycerol feeding regime was followed. Full details of GC–MS analyses for the sterol content obtained using comparable flask and fermenter cultures are given in the Supplementary materials (Tables S1 and S2 respectively). The sterol composition and yields from perdeuterated flask cultures and perdeuterated fed-batch fermenter cultures are shown in Fig. 3.

In the fermenter cultures, there was an immediate gain associated with the volumetric yield of cell paste, typically by a factor at least 10 (Haertlein et al., 2016). Furthermore, despite the fact that the sterol yield (per gram of cell paste) was lower in fermenter cultures, the fraction of d-cholesterol in the sterol pool was significantly higher (Fig. 3(b)), and facilitated subsequent purification.

3.4. Purification and characterisation by mass spectrometry of perdeuterated cholesterol

Starting with 31 g of perdeuterated cell paste grown in a fed-batch culture, the organic solvent extraction yielded 263 mg crude extract after solvent removal under reduced pressure. Purification using reverse-phase HPLC yielded 42.6 mg of perdeuterated cholesterol. The retention time of the perdeuterated cholesterol was 9.19 min. Purity of the isolated material was found to be 98.5% by both HPLC (detection wavelength 210 nm, data not shown) and GC–MS (see Fig. 4).

3.5. Evaluation of the potential of perdeuterated cholesterol in neutron reflectivity studies

The observed reflectivity data are shown in Fig. 5. Fits to these data were carried out using the Motofit software in Igor Pro (Nelson, 2010). The fitted thickness was 14.7 Å for the tail region, and 10.0 Å for the head region in all cases. Three different contrasts are shown in Fig 5: (i) perdeuterated cholesterol (d-cholesterol) and hydrogenated DPPC (h-DPPC) on null-reflecting water (NRW) (blue curve), (ii) unlabelled cholesterol (h-cholesterol) and d_{62}-DPPC on NRW (green curve), (iii) h-cholesterol and d_{62}-DPPC on D_2O (red curve). Contrast (i) allows the surface excess of cholesterol to be determined; contrast (ii) allows the surface excess of DPPC chains to be determined, and contrast (iii) allows the hydration of the head group layer to be determined.

The successful fitting of a common physical model to the data recorded for all three contrasts validates the surface excesses of the two components and the location of cholesterol at the interface. It is striking that the interpretation of the data from these measurements in terms of locating the cholesterol is rather straightforward. In the case of measurements on NRW, the reflectivity is strongly dominated by the deuterated material and this allows the location of the cholesterol molecules to be identified directly to be in the same region as the hydrocarbon tails of the lipid. The common physical model that is found to fit the data measured with three contrasts has the cholesterol in the same layer as the acyl chains of the DPPC. This is evident by examining the insert of Fig. 5, which shows the positioning of the cholesterol (blue line) within the region occupied by the acyl chains of the DPPC (green line). The phosphocholine head group region is effectively shown by the dip in the scattering length density (SLD) observed in the experiments performed with d_{62}-DPPC on D_2O, (red line in the insert of Fig. 5). The results thus show that the association of the molecules is mainly driven by hydrophobic interactions. An interfacial roughness of ~3.5 Å is required in the in the fit, as is shown by the non-abrupt changes in the density profiles between air, the two layers, and water. Another feature of the applied model is that there is no extensive penetration, beyond the OH group, of cholesterol towards the bulk water as its inclusion worsened the fit of the model to the measured data. This direct location of the cholesterol relies on the simple identification of these deuterated molecules. A fuller description of the analysis will be presented elsewhere and related to other results that have been reviewed by

Table 1b
Sterol composition of deuterated cholesterol-producing *P. pastoris* cell paste (mean values ± SD of triplicates are shown). Asterisks indicate the most likely sterol; identification is uncertain. Ergosterol was used as an internal standard (IS).

Peak	Compound	RT	Rel. (RT) (min)	Major mass peaks (silylated)	Peak area	% of total sterols	µg
1	Cholesterol	25.626	1.000	503, 488, (487), 411 (412), 393, 369, 133	885455935	50.8 ± 0.3	52 ± 10
2	Cholesta-5,8-dienol*	25.693	1.003	499, 389, 362	33293514	1.9 ± 0.0	2 ± 0
3	7-Dehydrocholesterol	26.262	1.025	499, 407, 389, 362	475750829	27.3 ± 0.1	28 ± 5
4	Zymosterol	26.472	1.033	499, 480, 389, 233, 78	85384591	4.9 ± 0.1	5 ± 1
5	Cholesta-5,7,14,24(25)-tetraenol*	26.874	1.049	495, 403, 385, 358	221871342	12.7 ± 0.2	13 ± 3
6	Cholesta-7,24(25)-dienol	26.995	1.053	499, 480, 369	28264322	1.6 ± 0.0	2 ± 0
7	Ergosterol (IS)	27.402	1.069	468, 378, 363, 337	174214398		10
8	not identified	27.961	1.091	496 (497, 498), 480, 352, 73	12625260	0.7 ± 0.1	1 ± 0
Total sterols		6.0 ± 0.7 mg/g CWW					

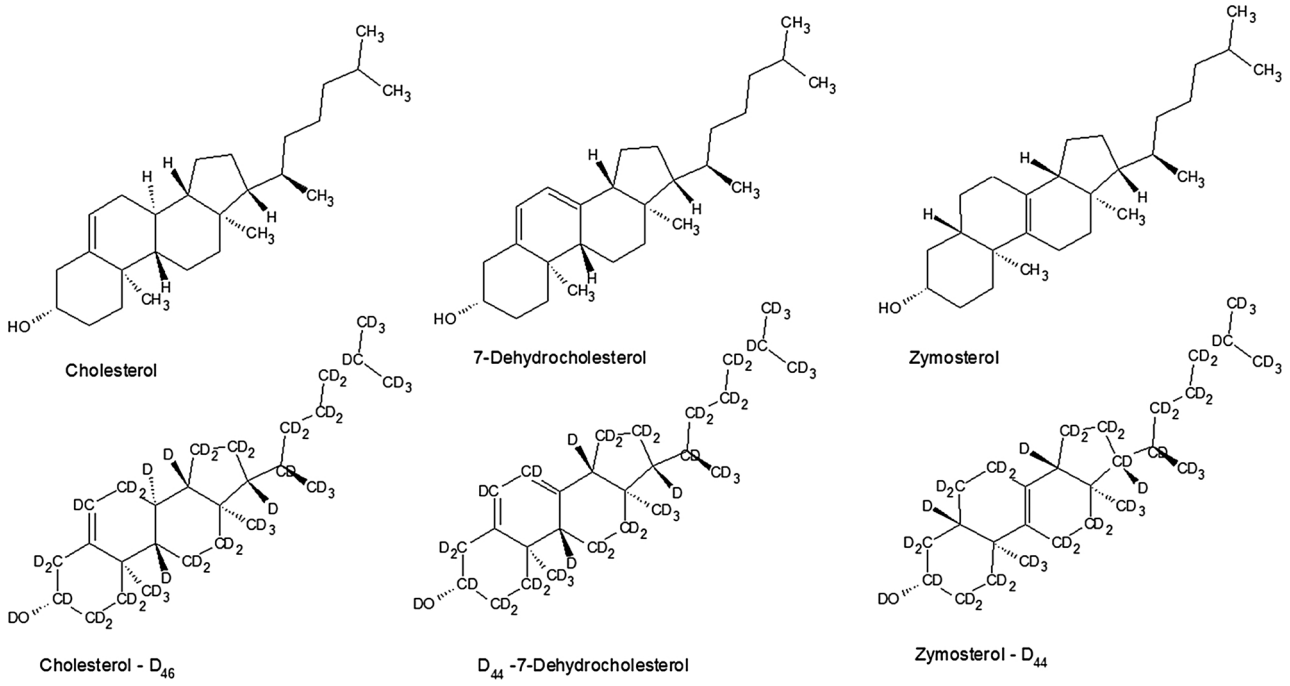

Fig. 2. Molecular structures of the main sterol species obtained through *in vivo* synthesis in unlabelled (top row) and perdeuterated (bottom row) flask cultures as identified by gas chromatography-mass spectrometry (GC–MS) analysis.

Rheinstädter and Mouritsen (2013). As the cholesterol is distributed over a considerable thickness(about the length of a cholesterol molecule), it is not possible to directly estimate an orientation or tilt of the molecules since the neutron reflection technique is sensitive only to the overall scattering length density distribution. Future diffraction studies of multiple bilayers that contain deuterated cholesterol could be helpful to give more information about the arrangement in three-dimensions.

4. Discussion

In neutron scattering experiments such as neutron reflection (NR) or small-angle neutron scattering (SANS), as well as in techniques such as NMR, deuterated membrane components provide important contrast when present in a mixture with other labelled or unlabelled lipids or when used to highlight membrane proteins. However, in common with perdeuterated proteins, perdeuterated cholesterol cannot be matched out in pure D_2O since its scattering length density is higher than that of D_2O. For protein labelling, protocols for match-out deuteration have been developed using *E. coli* or *P. pastoris* high cell-density cultures (Dunne et al., 2017) and protocols for match-out deuteration of cholesterol are currently undertaken in ILL's Life Sciences Group. As noted previously, the availability of d-cholesterol can be broadly exploited in neutron scattering studies – particularly those relating to lipid systems of various types. This capability is likely to provide novel information on the structural arrangement of mammalian membranes. Examples include small-angle neutron scattering (SANS) of solutions or neutron reflection measurements of interfacial systems that are of direct relevance to membranes and membrane proteins, high density lipoprotein/low density lipoprotein (HDL/LDL) exchange phenomena related to atherosclerosis (Browning et al., 2017), properties of alveolar

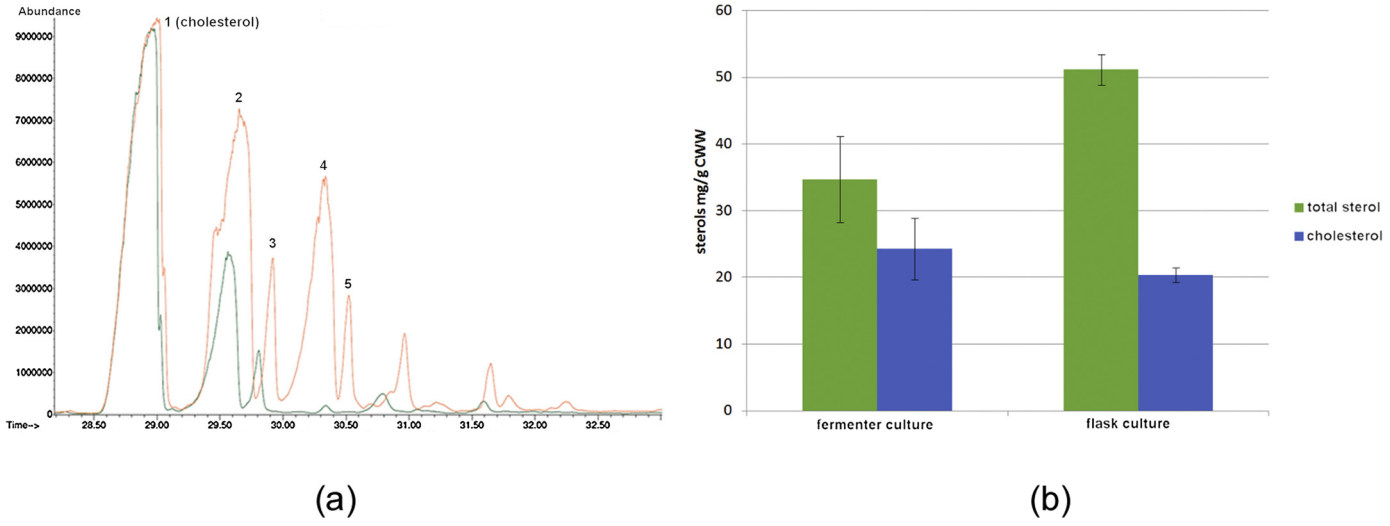

Fig. 3. (a) Main sterol components as analysed by GC–MS for the perdeuterated flask culture (red) and the fermenter culture (green) (b) total sterol content (green) and perdeuterated cholesterol (blue) produced in flask and in fermenter cultures. Mean values ± SD of triplicates are shown. (For interpretation of the references to colour in this figure legend, the reader is referred to the web version of this article.)

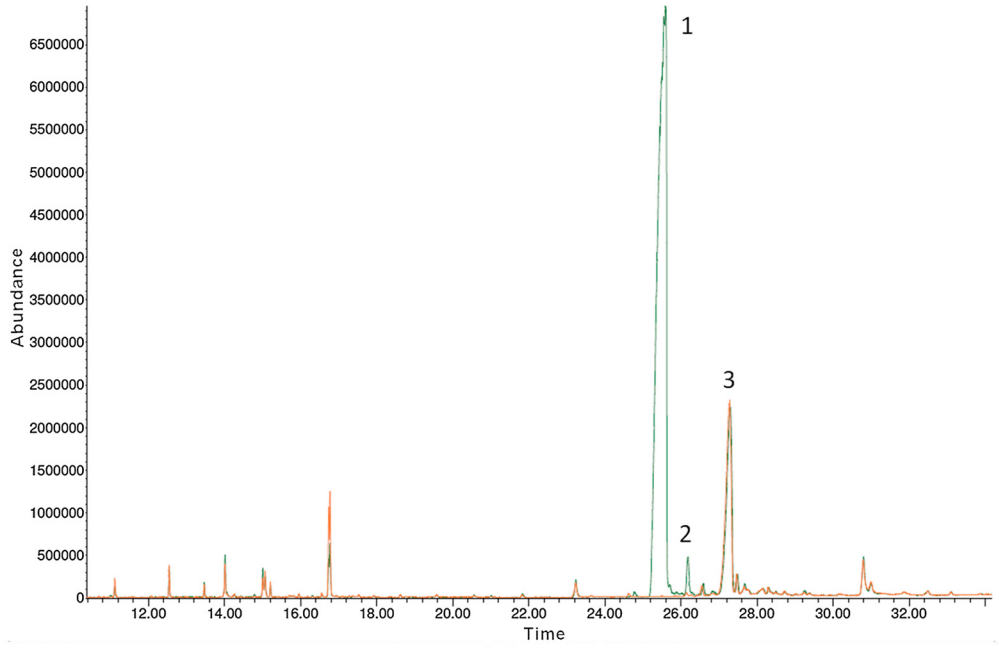

(a)

Compound	Peak no.	Retention time	Relative retention time	Area	%	µg
d-cholesterol	1	25.999	1.000	1078903796	98.4	53
Unknown sterol	2	26.183	1.023	17521750	1.6	0.9
Ergosterol (internal standard)	3	27.300	1.066	202006579		10

(b)

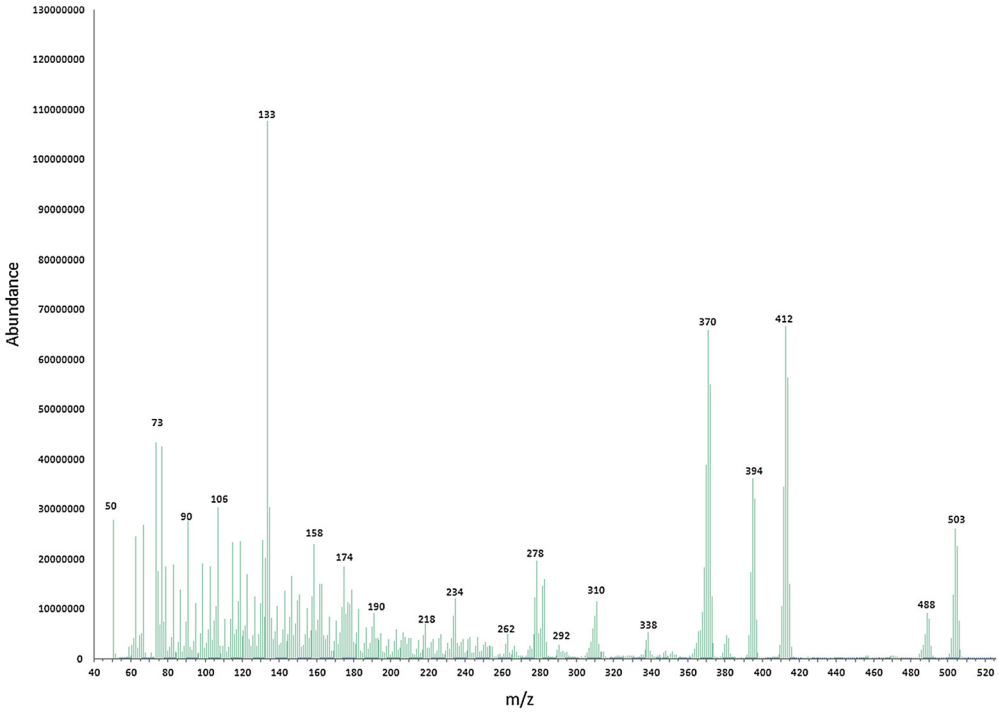

(c)

Fig. 4. Characterisation of purified perdeuterated cholesterol by gas chromatography-mass spectrometry (GC–MS) (a) showing the main peaks, including ergosterol as an internal standard (b) associated data extracted from GC–MS results (c) *m/z* plot of peak 1 as shown in 4(a).

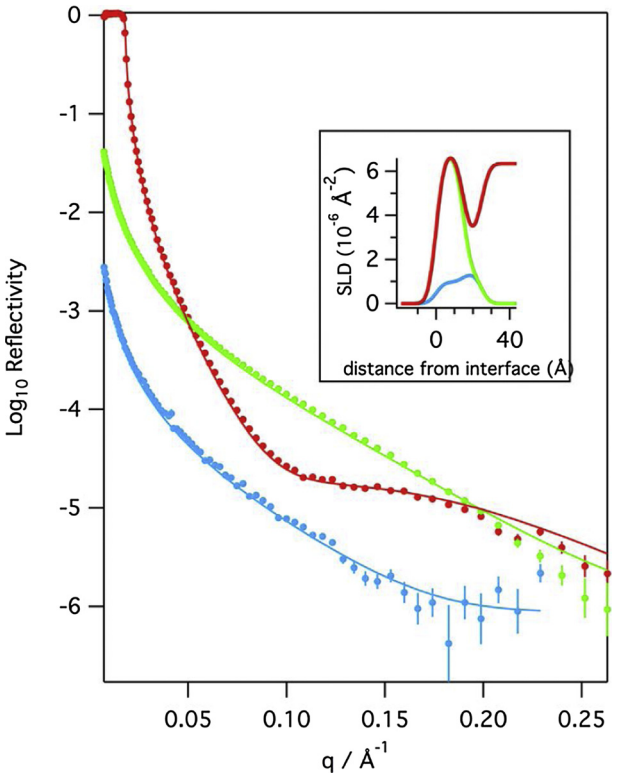

Fig. 5. Neutron reflectivity data for cholesterol:DPPC mixtures (1:4 molar ratio) at the air-water interface. Three different neutron contrasts are shown: perdeuterated cholesterol and h-DPPC on NRW (blue), unlabelled cholesterol and d_{62}-DPPC on NRW (green) and unlabelled cholesterol and d_{62}-DPPC on D_2O (red). The inset shows how the neutron scattering length density (SLD) varies with distance from the interface for the three different contrasts measured. (For interpretation of the references to colour in this figure legend, the reader is referred to the web version of this article.)

surfaces, and lung surfactant systems (Thompson et al., 2010, 2013; Hemming et al., 2015) where it is desirable to identify the physical and chemical changes of specific components. Other applications are possible in neutron crystallographic studies of proteins that interact with cholesterol, and neutron incoherent scattering studies that focus on the dynamics of specific components of a membranous system. Besides its use for neutron scattering and possibly for NMR applications, perdeuterated cholesterol, in combination with stimulated Raman scattering (SRS), could be extremely valuable in imaging approaches for the study of intracellular cholesterol trafficking mechanisms (Lee et al., 2015). The combination of microscopic information with Raman spectroscopy provides a powerful molecular imaging method, and allows visualization at the diffraction limit of the laser light used, and biochemical characterization through associated spectral information. In order to distinguish the molecules of interest from other naturally occurring biomolecules spectroscopically, deuterium labels are needed. The introduction of carbon-deuterium (C–D) bonds into biomolecules or drug compounds by *in vivo* deuteration approaches (Haertlein et al., 2016) or by organic synthesis (Bergner et al., 2011) is a relatively non-invasive labelling approach that does not cause major changes to the chemical and physiological properties of the molecules. In Raman imaging, C-deuterated molecules exhibit characteristic vibrational signatures in the C–D stretching region around 2100–2300 cm^{-1}, avoiding spectral interference with contributions from a complex biological environment. Raman microscopy, in combination with deuteration of fatty acids, has been used to image the metabolism of such lipids in macrophages and to trace their subsequent storage patterns. The appearance of cytosolic lipid droplets is a hallmark of macrophage transformation into foam cells, a key step in early atherosclerosis (Matthäus et al., 2012). Perdeuterated cholesterol may also be used for highly efficient screening of drugs that target cholesterol metabolism.

Low level deuterium incorporation from heavy water into fatty acids and cholesterol is an attractive method for determining their fractional synthesis in humans (Leitch and Jones, 1993). Diraison et al. (1996) found that the maximum *in vivo* incorporation number of deuterium atoms into plasma cholesterol was 27 out of the 46 hydrogen atoms present in the molecule. Since in mammals the toxicity of deuterium becomes evident at about 20% replacement of body water by deuterium oxide (Katz et al., 1962), full deuteration of cholesterol requires a recombinant expression system that can cope with high deuterium concentrations.

Acknowledgements

V.T.F. acknowledges support from the EPSRC under grant numbers GR/R99393/01 and EP/C015452/1 which funded the creation of the Deuteration Laboratory (D-Lab) in the Life Sciences group of the ILL. This work used the platforms of the Grenoble Instruct-ERIC Centre (ISBG; UMS 3518 CNRS-CEA-UGA-EMBL) with support from FRISBI (ANR-10-INSB-05-02) and GRAL (ANR-10-LABX-49-01) within the Grenoble Partnership for Structural Biology (PSB). G.A.S. acknowledges the support of this work by the Federal Ministry of Science, Research and Economy (BMWFW), the Federal Ministry of Traffic, Innovation and Technology (bmvit), the Styrian Business Promotion Agency SFG, the Standortagentur Tirol, the Government of Lower Austria and Business Agency Vienna through the COMET-Funding Program managed by the Austrian Research Promotion Agency FFG. The authors also thank Sandra Moser for support with GC–MS analysis and the ILL for the provision of beam time.

Appendix A. Supplementary data

Supplementary data associated with this article can be found, in the online version, at https://doi.org/10.1016/j.chemphyslip.2018.01.006.

References

Appolaire, A., Girard, E., Colombo, M., Durá, M.A., Moulin, M., Haertlein, M., Franzetti, B., Gabel, F., 2014. Small-angle neutron scattering reveals the assembly mode and oligomeric architecture of TET, a large, dodecameric aminopeptidase. Acta Crystallogr. D 70 (Pt. 11), 2983–2993.

Bergner, G., Albert, C.R., Schiller, M., Bringmann, G., Schirmeister, T., Dietzek, B., Niebling, S., Schlücker, S., Popp, J., 2011. Quantitative detection of C-deuterated drugs by CARS microscopy and Raman microspectroscopy. Analyst 136, 3686–3693.

Blakeley, M.P., Hasnain, S.S., Antonyuk, S.V., 2015. Sub-atomic resolution X-ray crystallography and neutron crystallography: promise, challenges and potential. IUCrJ 30, 464–474.

Braun, L., Uhlig, M., von Klitzing, R., Campbell, R.A., 2017. Polymers and surfactant at fluid interfaces studied with specular neutron reflectometry. Adv. Colloid Interface Sci. 247, 130–148.

Browning, K.L., Lind, T.K., Maric, S., Malekkhaiat-Haffner, S., Fredrikson, G.N., Bengtsson, E., Malmsten, M., Cárdenas, M., 2017. Human lipoproteins at model cell membranes: effect of lipoprotein class on lipid exchange. Sci. Rep. 7 (1), 7478.

Campbell, R.A., Wacklin, H.P., Sutton, I., Cubitt, R., Fragneto, G., 2011. FIGARO: The new horizontal neutron reflectometer at the ILL. Eur. Phys. J. Plus 126, 107.

Casadei, C.M., Gumiero, A., Metcalfe, C.L., Murphy, E.J., Basran, J., Concilio, M.G., Teixeira, S.C., Schrader, T.E., Fielding, A.J., Ostermann, A., Blakeley, M.P., Raven, E.L., Moody, P.C., 2014. Heme enzymes: neutron cryo-crystallography captures the protonation state of ferryl heme in a peroxidase. Science 345, 193–197.

Cuypers, M.G., Mason, S.A., Blakeley, M.P., Mitchell, E.P., Haertlein, M., Forsyth, V.T., 2013a. Near-atomic resolution neutron crystallography on perdeuterated *Pyrococcus furiosus* rubredoxin: implication of hydronium ions and protonation state equilibria in redox changes. Angew. Chem. 52 (3), 1022–1025.

Cuypers, M.G., Trubitsyna, M., Callow, P., Forsyth, V.T., Richardson, J.M., 2013b. Solution conformations of early intermediates in Mos1 transposition. Nucleic Acids Res. 41 (3), 2020–2033.

Cuypers, M.G., Mason, S.A., Mossou, E., Haertlein, M., Forsyth, V.T., Mitchell, E.P., 2016. Macromolecular structure phasing by neutron anomalous diffraction. Sci. Rep. 6, 31487.

de Ghellinck, A., Schaller, H., Laux, V., Haertlein, M., Sferrazza, M., Marechal, E., Wacklin, H., Jouhet, J., Fragneto, G., 2014. Production and analysis of perdeuterated lipids from *Pichia pastoris* cells. PLoS One 9 (4), e92999.

de Ghellinck, A., Fragneto, G., Laux, V., Haertlein, M., Jouhet, J., Sferrazza, M., Wacklin, H., 2015. Lipid polyunsaturation determines the extent of membrane structural

changes induced by Amphotericin B in *Pichia pastoris* yeast. BBA Biomembr. 1848, 2317–2325.
Diraison, F., Pachiaudi, C., Beylot, M., 1996. *In vivo* measurement of plasma cholesterol and fatty acid synthesis with deuterated water: determination of the average number of deuterium atoms incorporated. Metabolism 45 (7), 817–821.
Dunne, O., Weidenhaupt, M., Callow, P., Martel, A., Moulin, M., Perkins, S.J., Haertlein, M., Forsyth, V.T., 2017. Matchout deuterium labelling of proteins for small-angle neutron scattering studies using prokaryotic and eukaryotic expression systems and high cell-density cultures. Eur. Biophys. J. 46, 425–432.
Edlich-Muth, C., Artero, J.-B., Callow, P., Przewloka, M.R., Watson, A.A., Zhang, W., Glover, D.M., Debski, J., Dadlez, M., Round, A.R., Forsyth, V.T., Laue, E.D., 2015. The pentaplasmic nucleoplasmin fold is present in Drosophila FKBP39 and a large number of chromatin-related proteins. J. Mol. Biol. 427 (10), 1949–1963.
Foglia, F., Barlow, D.J., Szoka Jr., F.C., Huang, Z., Rogers, S.E., Lawrence, M.J., 2011. Structural studies of the monolayers and bilayers formed by a novel cholesterol-phospholipid chimera. Langmuir 27, 8275–8281.
Fragneto, G., 2012. Neutrons and model membranes. Eur. Phys. J. Special Top. 213 (1), 327–342.
Gerelli, Y., de Ghellinck, A., Jouhet, J., Laux, V., Haertlein, M., Fragneto, G., 2014. Multilamellar organization of fully deuterated lipid extracts of yeast membranes. Acta Crystallogr. D 70, 3167–3176.
Grage, S.L., Keleshian, A.M., Turdzeladze, T., Battle, A.R., Tay, W.C., May, R.P., Holt, S.A., Contera, S.A., Haertlein, M., Moulin, M., Pal, P., Rohde, P.R., Forsyth, V.T., Watts, A., Huang, K.C., Ulrich, A.S., Martinac, B., 2011. Bilayer-mediated clustering and functional interaction of MscL channels. Biophys. J . 100 (5), 1252–1260.
Haertlein, M., Moulin, M., Devos, J.M., Laux, V., Dunne, O., Forsyth, V.T., 2016. Biomolecular deuteration for neutron structural biology and dynamics. Methods Enzymol. 566, 113–157.
Hagn, F., Etzkorn, M., Raschle, T., Wagner, G., 2013. Optimized phospholipid bilayer nanodiscs facilitate high-resolution structure determination of membrane proteins. J. Am. Chem. Soc. 135 (5), 1919–1925.
Haupt, M., Blakeley, M.P., Fisher, S.J., Mason, S.A., Cooper, J.B., Mitchell, E.P., Forsyth, V.T., 2014. Binding site asymmetry in human transthyretin: insights from a joint neutron and X-ray crystallographic analysis using perdeuterated protein. IUCrJ 1, 429–438.
Hemming, J.M., Hughes, B.R., Rennie, A.R., Tomas, S., Campbell, R.A., Hughes, A.V., Arnold, T., Botchway, S.W., Thompson, K.C., 2015. Environmental pollutant ozone causes damage to lung surfactant protein b (SP-B). Biochemistry 54, 5185–5197.
Hirz, M., Richter, G., Leitner, E., Wriessnegger, T., Pichler, H., 2013. A novel cholesterol-producing *Pichia pastoris* strain is an ideal host for functional expression of human Na,K-ATPase α3β1 isoform. Appl. Microbiol. Biotechnol. 97 (21), 9465–9478.
Howard, E.I., Blakeley, M.P., Haertlein, M., Petit-Haertlein, I., Mitschler, A., Fisher, S.J., Cousido-Siah, A., Salvay, A.G., Popov, A., Muller-Dieckmann, C., Petrova, T., Podjarny, A., 2011. Neutron structure of type-III antifreeze protein allows the reconstruction of AFP-ice interface. J. Mol. Recognit. 24 (4), 724–732.
Ibrahim, Z., Martel, A., Moulin, M., Kim, H.S., Härtlein, M., Franzetti, B., Gabel, F., 2017. Time-resolved neutron scattering provides new insight into protein substrate processing by a AAA+ unfoldase. Sci. Rep. 7, 40948.
Katz, J.J., Crespi, H.L., Czajka, D.M., Finkel, A.J., 1962. Course of deuteriation and some physiological effects of deuterium in mice. Am. J. Physiol. 203, 907–913.
Kessner, D., Kiselev, M.A., Hauss, T., Dante, S., Wartewig, S., Neubert, R.H., 2008. Localisation of partially deuterated cholesterol in quaternary SC lipid model membranes: a neutron diffraction study. Eur. Biophys. J. 37 (6), 1051–1057.
Kwon, H., Basran, J., Casadei, C.M., Fielding, A.J., Schrader, T.E., Ostermann, A., Devos, J.M., Aller, P., Blakeley, M.P., Moody, P.C., Raven, E.L., 2016. Direct visualization of a Fe(IV)-OH intermediate in a heme enzyme. Nat. Commun. 7, 13445.
Lee, H.J., Zhang, W., Zhang, D., Yang, Y., Liu, B., Barker, E., Buhman, K.K., Slipchenko, L.V., Dai, M., Cheng, J.X., 2015. Assessing cholesterol storage in live cells and *C. elegans* by stimulated Raman scattering imaging of phenyl-Diyne cholesterol. Sci. Rep. 5, 7930.
Leitch, C.A., Jones, P.J., 1993. Measurement of human lipogenesis using deuterium incorporation. J. Lipid Res. 34, 157–163.
Lind, T.K., Wacklin, H., Schiller, J., Moulin, M., Haertlein, M., Pomorski, T.G., Cardenas, M., 2015. Formation and characterization of supported lipid bilayers composed of hydrogenated and deuterated *Escherichia coli* lipids. PLoS One 10 (12), e0144671.
Maric, S., Skar-Gislinge, N., Midtgaard, S., Thygesen, M.B., Schiller, J., Frielinghaus, H., Moulin, M., Haertlein, M., Forsyth, V.T., Pomorski, T.G., Arleth, L., 2014. Stealth carriers for low-resolution structure determination of membrane proteins in solution. Acta Crystallogr. D 70 (Pt. 2), 317–328.
Maric, S., Thygesen, M.B., Schiller, J., Marek, M., Moulin, M., Haertlein, M., Forsyth, V.T., Bogdanov, M., Dowhan, W., Arleth, L., Pomorski, T.G., 2015. Biosynthetic preparation of selectively deuterated phosphatidylcholine in genetically modified *Escherichia coli*. Appl. Microbiol. Biotechnol. 99 (1), 241–254.
Marsh, D., 2010. Molecular volumes of phospholipids and glycolipids in membranes. Chem. Phys. Lipids 163, 667–677.
Matthäus, C., Krafft, C., Dietzek, B., Brehm, B.R., Lorkowski, S., Popp, J., 2012. Noninvasive imaging of intracellular lipid metabolism in macrophages by Raman microscopy in combination with stable isotopic labelling. Anal. Chem. 84 (20), 8549–8556.
Micciulla, S., Gerelli, Y., Campbell, R.A., Schneck, E., 2018. A versatile method for the distance-dependent structural characterization of interacting soft interfaces by neutron reflectometry. Langmuir 34 (3), 789–800.
Nelson, A., 2010. Motofit–integrating neutron reflectometry acquisition, reduction and analysis into one, easy to use, package. J. Phys. Conf. Ser. 251, 012094.
Rheinstädter, M.C., Mouritsen, O.G., 2013. Small-scale structure in fluid cholesterol?lipid bilayers. Curr. Opin. Colloid Interface Sci. 18, 440–447.
Schirò, G., Fichou, Y., Gallat, F.-X., Wood, K., Gabel, F., Moulin, M., Härtlein, M., Heyden, M., Colletier, J.-P., Orecchini, A., Paciaroni, A., Wuttke, J., Tobias, D.J., Weik, M., 2015. Translational diffusion of hydration water correlates with functional motions in folded and intrinsically disordered proteins. Nat. Commun. 6, 6490.
Sheridan, A.J., Slater, J.M., Arnold, T., Campbell, R.A., Thompson, K.C., 2017. Changes to DPPC domain structure in the presence of carbon nanoparticles. Langmuir 33 (39), 10374–10384.
Small, D.M., 1984. Lateral chain packing in lipids and membranes. J. Lipid Res. 25, 1490–1500.
Stockton, G.W., Johnson, K.G., Butler, K.W., Tulloch, A.P., Boulanger, Y., Smith, I.C.P., Davis, J.H., Bloom, M., 1977. Deuterium NMR study of lipid organization in *Acholeplasma laidawii* membranes. Nature 269, 267–268.
Thompson, K.C., Rennie, A.R., King, M.D.S., Hardman, J.O., Lucas, C.O.M., Pfrang, C., Hughes, B.R., Hughes, A.V., 2010. Reaction of a phospholipid monolayer with gas-phase ozone at the air-water interface: measurement of surface excess and surface pressure in real time. Langmuir 26, 17295–17303.
Thompson, K.C., Jones, S.H., Rennie, A.R., King, M.D., Ward, A.D., Hughes, B.R., Lucas, C.O.M., Campbell, R.A., Hughes, A.V., 2013. Degradation and rearrangement of a lung surfactant lipid at the air-water interface during exposure to the pollutant gas ozone. Langmuir 29, 4594–4602.
Vijayakrishnan, S., Kelly, S.M., Gilbert, R.J.C., Callow, P., Bhella, D., Forsyth, V.T., Lindsay, J.G., Byron, O., 2010. Solution structure and characterisation of the human pyruvate dehydrogenase complex core assembly. J. Mol. Biol. 399, 71–93.